# Body-Centered Tetragonal $C_4$: A Viable $sp^3$ Carbon Allotrope

Koichiro Umemoto,[1] Renata M. Wentzcovitch,[2] Susumu Saito,[3] and Takashi Miyake[4]

[1]*Department of Geology and Geophysics, University of Minnesota, 421 Washington Avenue SE, Minneapolis, Minnesota 55455, USA*
[2]*Minnesota Supercomputing Institute and Department of Chemical Engineering and Materials Science, University of Minnesota, 421 Washington Avenue SE, Minneapolis, Minnesota 55455, USA*
[3]*Department of Physics, Tokyo Institute of Technology, 2-12-1 Oh-okayama, Meguro-ku, Tokyo 152-8551, Japan*
[4]*Research Institute for Computational Sciences, AIST, Umezono, Tsukuba 305-8568, Japan*

(Received 12 October 2009; revised manuscript received 27 January 2010; published 26 March 2010)

We have investigated by first principles the electronic, vibrational, and structural properties of bct $C_4$, a new form of crystalline $sp^3$ carbon recently found in molecular dynamics simulations of carbon nanotubes under pressure. This phase is transparent, dynamically stable at zero pressure, and more stable than graphite beyond 18.6 GPa. Coexistence of bct $C_4$ with $M$ carbon can explain better the x-ray diffraction pattern of a transparent and hard phase of carbon produced by the cold compression of graphite. Its structure appears to be intermediate between that of graphite and hexagonal diamond. These facts suggest that bct $C_4$ is an accessible form of $sp^3$ carbon along the graphite-to-hexagonal diamond transformation path.

DOI: 10.1103/PhysRevLett.104.125504 PACS numbers: 61.50.Ks, 61.48.De, 64.30.Jk, 71.20.Mq

Carbon nanotubes (CNT) [1] and fullerenes [2,3] are today fundamental building blocks in nanoscience and nanotechnology. They are used as one- and zero-dimensional structural units from which numerous complex nanostructures are synthesized. Compression of these nanostructures at high temperatures is a promising route for syntheses of new carbon phases with novel electronic and structural properties.

Theoretical studies are also indispensable in the search for new carbon allotropes. For instance, a joint effort between experiments and computations [4] was necessary to determine the polymerized forms of solid $C_{60}$ under pressure [5,6]. These resulting structures were very complex and contained large numbers of both $sp^2$ and $sp^3$ carbons. In the case of CNTs, up to now, crystalline solid CNT with uniform chirality has not been synthesized. Hence, it is still impossible to perform high pressure experiments on such crystals. A recent tight-binding molecular dynamics study produced new distinct phases by compressing various solid CNTs to different conditions [7]. Among them, a phase obtained by compression of a (10, 10) CNT lattice to 20 GPa is very intriguing. It consists of only $C_4$ square rings. Like diamond, it has only $sp^3$ carbons, despite being synthesized from a structure with $sp^2$ carbons. Its unit cell is body-centered tetragonal (bct) with four carbon atoms. Hereafter, we refer to this $sp^3$-carbon allotrope as bct $C_4$. Previously, bct $C_4$ was investigated theoretically to assess the stability of a crystal structure formed by small four-membered rings found in simulations of amorphous carbon [8]. In the present Letter, we investigate by first principles the structural, vibrational, and electronic properties of bct $C_4$. We also compare synthetic x-ray diffraction (XRD) patterns of this phase with those of a new phase produced by the cold compression of graphite [9].

The crystal structure of bct $C_4$ with the space group $I4/mmm$ is shown in Fig. 1. All carbon atoms are symmetrically equivalent; their Wyckoff position is $8h(x, x, 0)$. There are two kinds of bonds whose lengths are $d_1 = 2ax$ and $d_2 = \sqrt{2(2x - \frac{1}{2})a^2 + \frac{1}{4}c^2}$, where $a$ and $c$ are lattice constants. The structure of bct $C_4$ is closely related to those of graphite and hexagonal diamond. The view along the

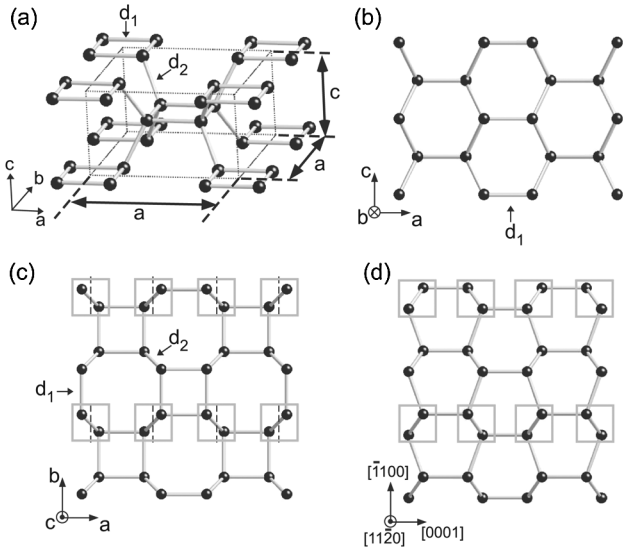


FIG. 1. Crystal structure of bct $C_4$: (a) three-dimentional view, (b) view along the $b$ axis, and (c) along the $c$ axis. In (c), if pairs of carbon atoms in the gray boxes are flipped across the planes denoted by dashed lines, bct $C_4$ transforms to (d) hexagonal diamond.

 

$a$ ($b$) axis of bct $C_4$ resembles that of the hypothetical $AA$-stacked graphite [Fig. 1(b)]. However, the layers are severely buckled and connected to each other. The view along the $c$ axis [Fig. 1(c)] shows that the hexagonal layers are stacked in the $AB$ sequence along the $a$ and $b$ axes. By rearranging half of carbon atoms, i.e., by changing the buckling pattern of these layers, bct $C_4$ can be transformed into hexagonal diamond [see Figs. 1(c) and 1(d) and the Fig. 1 caption].

Calculations of structural and vibrational properties were performed using the local-density approximation (LDA) [10,11]. The carbon pseudopotential was generated using Vanderbilt's method [12]. Cutoff radii for $2s$, $2p$, and $3d$ states are 1.3 a.u. The plane-wave cutoff energy is 50 Ry. We used variable-cell-shape molecular dynamics [13,14] for structural optimization under arbitrary pressure. The vibrational spectrum was obtained using density functional perturbation theory [15,16]. We computed the vibrational contribution to the free energies within quasiharmonic theory [17]. The numbers of $\mathbf{k}$ points and $\mathbf{q}$ points in the irreducible wedge used are 64 and 4, respectively. The quasiparticle spectrum (energy-band structures) was calculated using the $GW$ approximation (GWA) [18,19] for the zero pressure optimized structure. In particular, the GWA scheme we have used is implemented in the all-electron full potential linear muffin-tin orbital (FP-LMTO) method [20]. We use 13 MT orbitals per carbon to describe the valence wave functions in the MT spheres. Scalar relativistic effects and renormalization factors are included. Self-energies are calculated using LDA Kohn-Sham eigenvalues and eigenfunctions (one-shot $GW$).

The striking feature of bct $C_4$ is its relative stability with respect to other well-known carbon allotropes. At 0 GPa, bct $C_4$ is more stable than fcc solid $C_{60}$ [21] and as stable as (7,0) and (8,0) CNTs [22], while it is somewhat less stable than graphite, cubic diamond, and hexagonal diamond (Fig. 2). Phonon dispersions of bct $C_4$ indicate that it is dynamically stable over a wide pressure range, up to ~95 GPa [23]. Therefore, once synthesized, bct $C_4$ should be quenchable as a metastable phase to ambient pressure and low temperatures. Beyond 95 GPa, a zone-edge soft mode appears, and bct $C_4$ distorts into a primitive tetragonal phase with 8 carbon atoms in the unit cell [23]. The static structural parameters of bct $C_4$ at 0 GPa are $a = 4.329$ Å, $c = 2.483$ Å, and $x = 0.1804$. The two distinct bond lengths, $d_1$ and $d_2$, are 1.562 and 1.506 Å, respectively. These values are longer and shorter, respectively, than the bond length in diamond, 1.54 Å. The equation of state parameters of bct $C_4$ and those of other carbon allotropes are given in Table I. Its equilibrium volume is ~6% larger than diamond's and its bulk modulus is ~7% smaller. Nonetheless, bct $C_4$ is rather incompressible compared with cubic boron-nitride [27,28].

The electronic band structure of bct $C_4$ is shown in Fig. 3. It is insulating with an indirect band gap. The valence band top is at the $Z$ point and the conduction band bottom is along the $\Lambda$ line. The LDA band gap is 2.56 eV, being quite smaller than diamond's. The GWA correction to the LDA value does not change the band structure qualitatively, but increases the band gap to 3.78 eV. While LDA tends to underestimate the band gap width considerably, GWA is known to predict band gaps very close to experimental values for this class of materials [19]. Therefore, bct $C_4$ should be optically transparent.

Under pressure, bct $C_4$ becomes stable with respect to graphite beyond 18.6 GPa (Fig. 2). Hence, this phase could be a by-product of some metastable pressure-induced phase transformations from graphite. It is known that

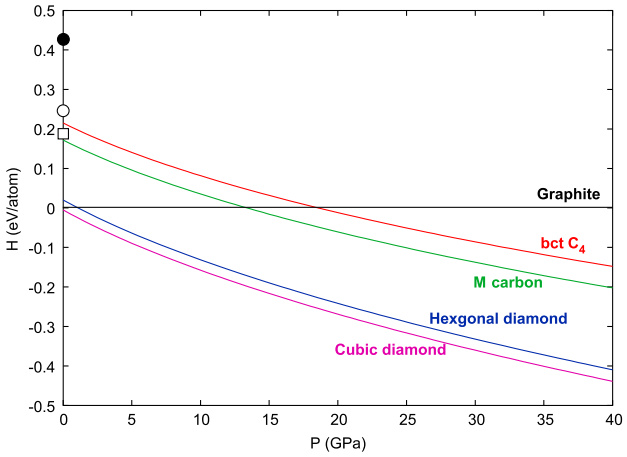


FIG. 2 (color online). Relative enthalpies of bct $C_4$, $M$ carbon, hexagonal diamond, and cubic diamond with respect to graphite. Black circle, white circle, and white squares represent enthalpies of fcc solid $C_{60}$ [21], (7,0) CNT, and (8,0) CNT [22], respectively.

TABLE I. Calculated equation of state parameters (Birch-Murnaghan) of bct $C_4$, cubic and hexagonal diamonds, $M$ carbon, and cubic boron-nitride (BN).

| At 0 GPa | $V_0$ (Å$^3$/atom) | $B_0$ (GPa) | $B_0'$ |
|---|---|---|---|
| bct $C_4$ (static) | 5.82 | 428.7 | 3.57 |
| bct $C_4$ (300 K) | 5.88 | 418.2 | 3.58 |
| Diamond (static) | 5.51 | 459.4 | 3.72 |
| Diamond (300 K) | 5.57 | 447.0 | 3.74 |
| Diamond (static[a]) | 5.52 | 468.5 | |
| Diamond (static[b]) | 5.483 | 458 | 3.70 |
| Diamond (exp.[c]) | 5.67 | 446 | 3.0 |
| $M$ carbon (static) | 5.77 | 428.9 | 3.58 |
| $M$ carbon (300 K) | 5.84 | 417.8 | 3.45 |
| $M$ carbon (static[d]) | 5.78 | 431.2 | |
| $M$ carbon (static[e]) | 5.745 | 422 | 3.77 |
| Cubic BN (exp.[f]) | 5.91 | 369 | 4.0 |
| Cubic BN (exp.[g]) | 5.91 | 387 | 3.06 |

[a]Reference [24]. [b]Reference [25], LDA. [c]Reference [26]. [d]Reference [24]. [e]Reference [25], LDA. [f]Reference [27]. [g]Reference [28].

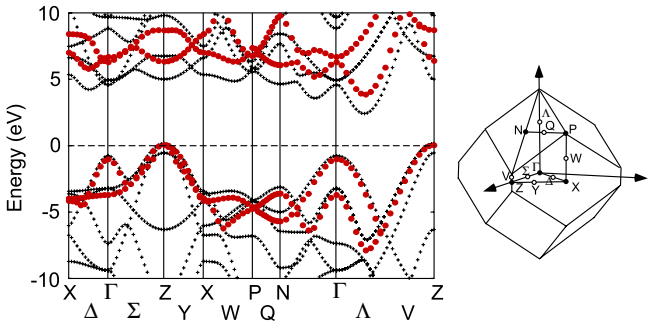


FIG. 3 (color online). Electronic band structures of bct $C_4$ at 0 GPa calculated using LDA (small crosses) and GWA (large circles). Energy is measured from the valence top. The figure on the right shows the first Brillouin zone of the bct lattice.

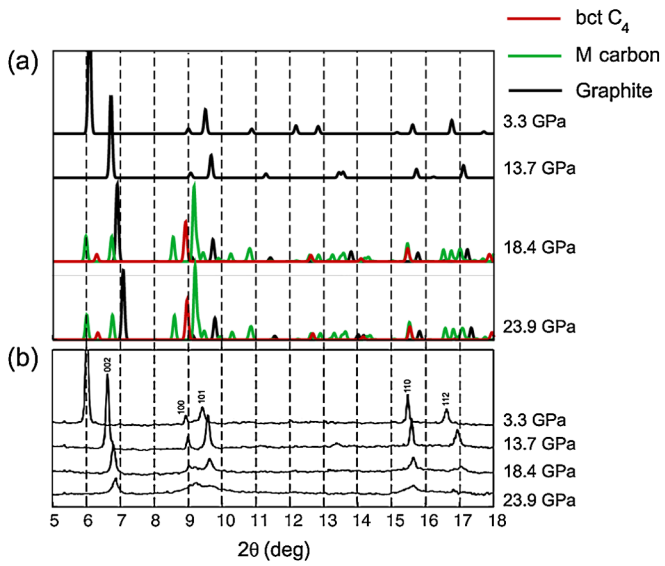


FIG. 4 (color online). (a) Simulated XRD patterns of bct $C_4$, graphite, and $M$ carbon. (b) Experimental XRD patterns [9]. X-ray wavelength is 0.3329 Å.

compression of graphite at room temperature produces a transparent phase with high electric resistivity [29–37], indicating a metal-insulator transition. This transparent phase is hard enough to scratch diamond [9] and is quenchable to atmospheric pressure at low temperatures [37]. This transformation is accompanied by broadening of some XRD peaks [9]. The properties of bct $C_4$ are consistent with all these observations.

Several other structures have been theoretically proposed to explain the behavior of the transition of graphite to the transparent phase under pressure. Ribeiro *et al.* studied several forms of hybrid diamond-graphite structures [38]. Among them, the $(3,0)/(4,0)$ and the $(3,0)/(4,0)ab$ phases were found to have lower enthalpies than graphite under pressure. The $(3,0)/(4,0)$ phase had the lower enthalpy than the $(3,0)/(4,0)ab$ phase. But the former is metallic and cannot be a candidate of the transparent phase. The latter is insulating and rather hard ($B_0$ is 411 GPa), while its simulated XRD pattern could not fully explain the experimental one. Very recently, $M$ carbon was proposed as a likely candidate [24]. It has lower enthalpy than the $(3,0)/(4,0)$ and the $(3,0)/(4,0)ab$ phases and should be transparent with a wide band gap. Its simulated $K$-edge spectra and XRD pattern agreed well with experimental ones. Enthalpy of bct $C_4$ is between those of transparent $M$ carbon and the $(3,0)/(4,0)ab$ phases; enthalpy of bct $C_4$ at 0 GPa is higher by 0.043 eV/atom than $M$ carbon and lower by 0.018 eV/atom than the $(3,0)/(4,0)ab$ phase. Enthalpy difference between these phases is not so large. A Raman experiment on graphite showed that its spectrum became similar to amorphous carbon at 37.6 GPa [39]. This may suggest a transition of graphite under pressure to a mixture of several transparent metastable phases, i.e., a transition to primary $M$ carbon with a small amount of bct $C_4$ and the $(3,0)/(4,0)ab$ phase. It is consistent with very broad peaks in the experimental XRD pattern of cold-compressed graphite at 23.9 GPa [9]. Figure 4 shows the simulated XRD patterns of graphite, $M$ carbon, and bct $C_4$ and compares them with experimental ones at various pressures. Coexistence of bct $C_4$ and $M$ carbon seems to explain better the observed broadenings of the 100 (at $2\theta \sim 9°$) and 110 (at $2\theta \sim 15.5°$) diffraction peaks.

Compression of graphite between ~1000 K and ~2000 K produces mixtures of hexagonal and cubic diamonds [30,33,36,40]. Above ~2000 K, only the stable cubic form is obtained. Therefore the metastable hexagonal form should be more accessible than the cubic form from graphite at lower temperature. Similarly, MD simulations have showed that the (10,10) CNT lattice transforms to graphite at 10 GPa, while at 20 GPa it transforms to two distinct phases, bct $C_4$ and hexagonal diamond [7]. Since bct $C_4$ has higher enthalpy than hexagonal diamond it is likely to transform to the latter by annealing. Therefore, bct $C_4$ is expected to be an intermediate phase along the transition path from graphite to hexagonal diamond. Its structural relationship to graphite and hexagonal diamond strongly supports this concept.

Bct $C_4$ can also be viewed as a polymerized form of (2,2) CNT consisting of eight-membered $sp^3$-carbon rings stacked along its $c$ axis [see Fig. 1(c)]. (2,2) CNT is known to be one of the two smallest stable $sp^3$ CNTs [41]. Bct $C_4$ is precisely solid (2,2) CNT interconnected by four-membered carbon squares. The other smallest stable CNT is (3,0) CNT. Its polymerized form is none other than hexagonal diamond.

There is an interesting analogy between the crystal structures of $H_2O$ ice and those of $sp^3$ carbon. By focusing on the hydrogen-bond network only, one can see that ice $I_h$ and $I_c$ are isostructural to hexagonal and cubic diamonds, respectively. In fact, a molecular dynamics simulation has shown that $H_2O$ molecules form a hydrogen-bond network consisting of eight-membered and four-membered $H_2O$

rings on the surface of hydroxylated $\beta$ cristobalite [42]. This $H_2O$ network is analogous to the bct $C_4$ structure.

The likelihood of growing bct $C_4$ on the surface of $\beta$ cristobalite is probably small, because of bondlength mismatch. However, bct $Sn_4$ and bct $Ge_4$ might grow more easily. The bond lengths of diamond-type Sn (2.81 Å) and Ge (2.45 Å) are much more similar to that of ice $I_h$ (2.75 Å) than the bond length of diamond (1.54 Å). Indeed, calculations have shown that the stability of bct $Ge_4$ tends to increase with respect to that of diamond-type Ge at expanded volumes (negative pressures) [43]. Therefore, it might be possible to stabilize bct $Ge_4$ on the surface of $\beta$ cristobalite.

In conclusion, the results and the structural relationships discussed in this Letter suggest that the structure of bct $C_4$ is another likely form of metastable and accessible fourfold-coordinated $sp^3$ system.

Calculations have been done using the quantum-ESPRESS package [44]. Research was supported by NSF Grants No. ATM-0426757 (VLab). S. S. acknowledges the support from the *Nanoscience and Quantum Physics* project of the Tokyo Institute of Technology through the Global Center of Excellence Program of the MEXT, Japan. Computations were performed at the Minnesota Supercomputing Institute.

[1] S. Iijima, Nature (London) **354**, 56 (1991).
[2] W. Krätschmer *et al.*, Nature (London) **347**, 354 (1990).
[3] K. Kikuchi *et al.*, Nature (London) **357**, 142 (1992).
[4] C. H. Xu and G. E. Scuseria, Phys. Rev. Lett. **74**, 274 (1995).
[5] M. Nunez-Regueiro *et al.*, Phys. Rev. Lett. **74**, 278 (1995).
[6] Y. Iwasa *et al.*, Science **264**, 1570 (1994).
[7] Y. Omata *et al.*, Physica (Amsterdam) **29E**, 454 (2005).
[8] P. A. Schultz, K. Leung, and E. B. Stechel, Phys. Rev. B **59**, 733 (1999).
[9] From W. L. Mao *et al.*, Science **302**, 425 (2003). Reprinted with permission from AAAS.
[10] D. M. Ceperley and B. J. Alder, Phys. Rev. Lett. **45**, 566 (1980).
[11] J. P. Perdew and A. Zunger, Phys. Rev. B **23**, 5048 (1981).
[12] D. Vanderbilt, Phys. Rev. B **41**, R7892 (1990).
[13] R. M. Wentzcovitch, Phys. Rev. B **44**, 2358 (1991).
[14] R. M. Wentzcovitch, J. L. Martins, and G. D. Price, Phys. Rev. Lett. **70**, 3947 (1993).
[15] P. Giannozzi *et al.*, Phys. Rev. B **43**, 7231 (1991).
[16] S. Baroni *et al.*, Rev. Mod. Phys. **73**, 515 (2001).
[17] D. Wallace, *Thermodynamics of Crystals* (Wiley, New York, 1972); P. Carrier, J. F. Justo, and R. M. Wentzcovitch, Phys. Rev. B **78**, 144302 (2008).
[18] L. Hedin, Phys. Rev. **139**, A796 (1965); L. Hedin and S. Lundqvist, in *Solid State Physics*, edited by H. Ehrenreich, F. Seitz, and D. Turnbull (Academic, New York, 1969), Vol. 23, p. 1.
[19] M. S. Hybertsen and S. G. Louie, Phys. Rev. Lett. **55**, 1418 (1985).
[20] T. Kotani and M. van Schilfgaarde, Solid State Commun. **121**, 461 (2002).
[21] S. Okada and S. Saito, Phys. Rev. B **59**, 1930 (1999).
[22] K. Kanamitsu and S. Saito, J. Phys. Soc. Jpn. **71**, 483 (2002).
[23] See supplementary material at http://link.aps.org/supplemental/10.1103/PhysRevLett.104.125504 for dynamical stability at low pressure and pressure-induced instability at 95 GPa.
[24] Q. Li *et al.*, Phys. Rev. Lett. **102**, 175506 (2009).
[25] Y. Liang, W. Zhang, and L. Chen, Europhys. Lett. **87**, 56003 (2009).
[26] F. Occelli, P. Loubeyre, and R. Letoullec, Nature Mater. **2**, 151 (2003).
[27] E. Knittle *et al.*, Nature (London) **337**, 349 (1989).
[28] A. F. Goncharov *et al.*, Phys. Rev. B **75**, 224114 (2007).
[29] R. B. Aust and H. G. Drickamer, Science **140**, 817 (1963).
[30] F. P. Bundy and J. S. Kasper, J. Chem. Phys. **46**, 3437 (1967).
[31] A. F. Goncharov, I. N. Makarenko, and S. M. Stishov, Sov. Phys. JETP **69**, 380 (1989).
[32] M. Hanfland, K. Syassen, and R. Sonnenschein, Phys. Rev. B **40**, 1951 (1989).
[33] W. Utsumi and T. Yagi, Science **252**, 1542 (1991); T. Yagi *et al.*, Phys. Rev. B **46**, 6031 (1992).
[34] K. J. Takano, H. Harashima, and M. Wakatsuki, Jpn. J. Appl. Phys. **30**, L860 (1991).
[35] Y. X. Zhao and I. L. Spain, Phys. Rev. B **40**, 993 (1989).
[36] F. P. Bundy *et al.*, Carbon **34**, 141 (1996).
[37] E. D. Miller, D. C. Nesting, and J. V. Badding, Chem. Mater. **9**, 18 (1997).
[38] F. J. Ribeiro *et al.*, Phys. Rev. B **72**, 214109 (2005).
[39] A. F. Goncharov, JETP Lett. **51**, 418 (1990).
[40] T. Irifune *et al.*, Nature (London) **421**, 599 (2003); T. Irifune *et al.*, Phys. Earth Planet. Inter. **143–144**, 593 (2004).
[41] D. Stojkovic, P. Zhang, and V. H. Crespi, Phys. Rev. Lett. **87**, 125502 (2001).
[42] J. Yang *et al.*, Phys. Rev. Lett. **92**, 146102 (2004).
[43] Y. Fujimoto *et al.*, New J. Phys. **10**, 083001 (2008).
[44] P. Giannozzi *et al.*, J. Phys. Condens. Matter **21**, 395502 (2009), http://www.quantum-espresso.org.